Neurobiology of Aging 42 (2016) 177–188

Contents lists available at ScienceDirect

Neurobiology of Aging

journal homepage: www.elsevier.com/locate/neuaging

Accelerated decline in white matter integrity in clinically normal individuals at risk for Alzheimer's disease

Anna Rieckmann [a,b], Koene R.A. Van Dijk [a,c], Reisa A. Sperling [a,d,e], Keith A. Johnson [d,e,f,g], Randy L. Buckner [a,c,g,h], Trey Hedden [a,g,*]

[a] Athinoula A. Martinos Center for Biomedical Imaging, Department of Radiology, Massachusetts General Hospital, Charlestown, MA, USA
[b] Department of Radiation Sciences, Diagnostic Radiology, Umeå University, Umeå, Sweden
[c] Department of Psychology and Center for Brain Science, Harvard University, Cambridge, MA, USA
[d] Department of Neurology, Massachusetts General Hospital, Harvard Medical School, Boston, MA, USA
[e] Center for Alzheimer Research and Treatment, Department of Neurology, Brigham and Women's Hospital, Harvard Medical School, Boston, MA, USA
[f] Division of Nuclear Medicine and Molecular Imaging, Department of Radiology, Massachusetts General Hospital, Harvard Medical School, Boston, MA, USA
[g] Department of Radiology, Massachusetts General Hospital, Harvard Medical School, Boston, MA, USA
[h] Department of Psychiatry, Massachusetts General Hospital, Harvard Medical School, Boston, MA, USA

ARTICLE INFO

Article history:
Received 7 September 2015
Received in revised form 13 March 2016
Accepted 14 March 2016
Available online 21 March 2016

Keywords:
Aging
Amyloid
Diffusion tensor imaging
Longitudinal
White matter

ABSTRACT

Prior studies have identified white matter abnormalities in Alzheimer's disease (AD). Yet, cross-sectional studies in normal older individuals show little evidence for an association between markers of AD risk (APOE4 genotype and amyloid deposition), and white matter integrity. Here, 108 normal older adults (age, 66–87) with assessments of apolipoprotein e4 (APOE4) genotype and assessment of amyloid burden by positron emission tomography underwent diffusion tensor imaging scans for measuring white matter integrity at 2 time points, on average 2.6 years apart. Linear mixed-effects models showed that amyloid burden at baseline was associated with steeper decline in fractional anisotropy in the parahippocampal cingulum ($p < 0.05$). This association was not significant between baseline measures suggesting that longitudinal analyses can provide novel insights that are not detectable in cross-sectional designs. Amyloid-related changes in hippocampus volume did not explain the association between amyloid burden and change in fractional anisotropy. The results suggest that accumulation of cortical amyloid and white matter changes in parahippocampal cingulum are not independent processes in individuals at increased risk for AD.

1. Introduction

Damage to white matter, including demyelination and axonal loss, is a frequent observation in postmortem examinations of patients with Alzheimer's disease (AD), and histopathological studies have shown that microstructural white matter damage in AD can occur independent of gray matter neurodegeneration (e.g., Bartzokis et al., 2004; Brun and Englund, 1986; Englund et al., 1988; Han et al., 2002).

Reduced integrity of white matter in AD has also been found with human in vivo magnetic resonance imaging (MRI) studies. These studies suggest a predominance of AD-related changes in the parietal and temporal white matter (e.g., Bozzali et al., 2002; Brickman et al., 2012; Head et al., 2004; Medina et al., 2006). Consistent with AD pathology and the notion of AD as a "disconnection" disorder (Hyman et al., 1984), analyses of specific fiber tracts using diffusion tensor imaging (DTI) have refined these results to identify a pronounced reduction of fractional anisotropy (FA) and increases in diffusivity in the parahippocampal cingulum, a collection of fibers which connect the hippocampal formation and the posterior cingulate cortex. Several studies have reported reduced parahippocampal white matter integrity already in mild cognitive impairment and normal individuals with cognitive complaints, and suggested this fiber bundle may play an important role in declining memory functions in the path to AD (Ito et al., 2015; Wang et al., 2012; Zhang et al., 2007). Further reductions in FA and increases in diffusivity in AD have been noted in nearby white matter pathways including the main cingulum bundle, the corpus callosum and the superior longitudinal fasciculi (e.g., Rose et al., 2000; Salat et al., 2010).

Elevated amyloid burden measured with positron emission tomography (PET) imaging of 11C-Pittsburgh Compound B (PIB) is a

* Corresponding author at: Athinoula A. Martinos Center for Biomedical Imaging, 149 13th Street, Charlestown, MA 02129. Tel.: +1-617-643-5529; fax: +1-617-726-7422.
E-mail address: hedden@nmr.mgh.harvard.edu (T. Hedden).

0197-4580/$ – see front matter © 2016 Elsevier Inc. All rights reserved.
http://dx.doi.org/10.1016/j.neurobiolaging.2016.03.016

biomarker of amyloid plaques, a neuropathological hallmark of AD, and is detectable in a subset of clinically normal older adults (Klunk, 2011; Rabinovici and Jagust, 2009; Sojkova and Resnick, 2011). Despite reliable associations between AD diagnosis and reduced white matter integrity, in the subset of clinically normal older adults with amyloid burden, evidence for white matter damage is inconsistent. Heightened amyloid deposition in older adults without AD diagnosis has been associated with subtle decreases (Chao et al., 2013), but also with paradoxical increases in FA, and no changes in diffusivity, in the medial temporal lobe, cingulum and corpus callosum (Racine et al., 2014), as well as no differences in FA, unless accompanied by gray matter neurodegeneration (Kantarci et al., 2014). Similarly, large white matter lesions observed as white matter hyperintensities (WMH) on T2-weighted MRI that are elevated in AD (Brickman, 2013, for review; Scheltens et al., 1995) show no association with amyloid burden in clinically normal individuals (e.g., Hedden et al., 2012; Marchant et al., 2012; Rutten-Jacobs et al., 2011; Vemuri et al., 2015). There is also little evidence that the presence of the apolipoprotein e4 (APOE4) allele is reliably associated with reduced FA in large samples of clinically normal older adults (Nyberg and Salami, 2014; Westlye et al., 2012), although it is a major risk factor for amyloid accumulation (Ossenkoppele et al., 2015) and AD (Corder et al., 1993). Notably, widespread increases in diffusivity for e4 carriers were noted in some studies, suggesting that diffusivity measures may be more sensitive to subtle white matter changes in healthy individuals at increased risk for AD (Heise et al., 2011; Westlye et al., 2012; but see; Nyberg and Salami, 2014).

Collectively, the previously mentioned observations provide mixed evidence for an association between markers of AD risk and imaging-based measures of white matter integrity in clinically normal older adults. It is possible that white matter tract disruption may emerge relatively late in the cascade of detectable biomarkers and may only become apparent when following individuals over time.

A major advantage of longitudinal studies is that within-person change can be directly examined instead of relying on the inference of age-related change through between-person comparisons. Longitudinal DTI studies have demonstrated that DTI measures are reliable within older individuals (Jovicich et al., 2014) and that white matter integrity shows significant decline in clinically normal older adults at a rate of approximately 0.5–1.0% per year for FA (Barrick et al., 2010; Charlton et al., 2010; Sexton et al., 2014; Teipel et al., 2010). The estimates of longitudinal change in FA have been shown to exceed those from cross-sectional designs, which could point to a positive selection bias for very old adults in cross-sectional studies (Charlton et al., 2010; Lövdén et al., 2014). One recent DTI study found markedly different associations between age-related declines in FA and a third variable (here, change in cognition) depending on whether age associations with FA were estimated longitudinally or cross-sectionally (Lövdén et al., 2014), and another study reported little convergence between cross-sectional and longitudinal age associations in a sample of adults between 19 and 78 years (Bender and Raz, 2015).

The present study revisits the question of when changes in white matter microstructure occur in individuals at increased risk for developing AD by examining longitudinally measured DTI metrics in clinically normal individuals with elevated amyloid burden. We predict that, even though associations between amyloid burden and white matter tract disruption are not always detectable cross-sectionally, they emerge when following individuals at increased risk for AD over time. The analyses are based on linear mixed-effects models with APOE4 status and amyloid burden as estimated by PET at baseline as predictors of longitudinal change in regional FA and diffusivity over an average duration of 2.6 years. In the analyses, we control for possible confounding effects such as age, sex, and head motion during MR imaging and investigate the influence of WMH on the association between markers of AD risk and longitudinal decline in DTI measures of white matter integrity. Informed by a significant finding in the parahippocampal cingulum, we also perform an additional analysis in which we investigate the relation between amyloid and hippocampal atrophy and whether an association between amyloid burden and FA in the parahippocampal cingulum is independent of this cascade.

2. Materials and methods

2.1. Sample

Participants were recruited as part of the Harvard Aging Brain Study, an ongoing longitudinal study. A total of 254 clinically normal older participants (Clinical Dementia Rating [CDR] = 0, mini mental-state examination score [MMSE] $\geq$ 26) with complete DTI data, structural MRI data, a ^{11}C-PiB PET scan, and APOE genotyping at baseline entered the study. Of these, 117 participants completed a second MRI exam 2.6 years later (range = 2.3–3.3). After exclusion of DTI data due to excessive head motion during a DTI scan (average motion exceeded 2.0 mm), 247 participants were included at baseline of which 108 had longitudinal DTI and structural MRI data. Where appropriate, we occasionally refer to the entire baseline sample for comparisons (Supplement 1 and 2). The main analyses and results are focused on longitudinal data from the 108 participants (61 women; mean age at baseline = 73.7, range = 66–87 years; mean education = 16.5 years, range = 8–20; mean MMSE at baseline = 29.1, range = 26–30; mean MMSE at follow-up = 29.3, range = 27–30). Subjects with a history of neurological or psychiatric disease or who were found ineligible for MRI were not allowed into the study. Based on self-report, 65 individuals had received a diagnosis and treatment of hypertension by their physician. In addition, a radiologist reviewed MRI images to rule out cortical infarcts, tumor, or other brain abnormalities. At follow-up, 12 individuals had changed from 0 to 0.5 on the CDR.

Allelic variation in the APOE gene was assessed by genotyping, and participants were grouped by the presence of at least one APOE e4 allele (N = 247: 25.5% e4+; N = 108: 28.7% e4+). None of the e4 carriers carried an APOE e2 allele. All participants gave written informed consent.

2.2. Amyloid imaging

PET images were acquired with an HR+ (CTI, Knoxville, TN, USA) PET camera at Massachusetts General Hospital (3D mode, 63 adjacent slices of 2.4 mm interval, 15.2-cm axial field of view, 5.6-mm transaxial resolution). Approximately 15-mCi 11C-PiB were intravenously administered as a bolus over 20–30 seconds. Dynamic images were acquired in 39 frames of increasing duration for a total of 60 minutes (8 $\times$ 5 seconds, 4 $\times$ 1 minute, 27 $\times$ 2 minutes). PET data were reconstructed using a filtered back-projection algorithm. Before the emission scans, a transmission scan of 10 minutes was performed, and photon attenuation measurements were used to correct the emission data. The participant's head was stabilized using a beaded cushion and velcro straps, and correction for residual head motion was performed on the dynamic data by registration to a common reference frame.

Dynamic data from the first 8 minutes were averaged to create an initial uptake image. The initial uptake image was used for normalization of native PET space to a standard PET template in Montreal Neurological Institute (MNI) space. Then, emission data were coregistered to standard space using the normalization

parameters obtained from the initial uptake image. Spatial normalizations were performed in SPM8 by a 2-step procedure of an initial 12-parameter affine transformation followed by nonlinear warping (http://www.fil.ion.ucl.ac.uk/spm/software/spm8/). Logan graphical analysis with cerebellar cortex as reference region was used on the normalized data to determine the distribution volume ratio (DVR, Logan et al., 1990; Price et al., 2005) for a large cortical region of interest (ROI). This volume consisted of frontal, lateral, and retrosplenial brain areas (frontal, lateral and retrosplenial brain region), defined as an aggregate of 60 Anatomical Automatic Labeling regions, and was used to obtain a summary measure of amyloid burden (e.g., Gomperts et al., 2008; Hedden et al., 2009, 2012; Johnson et al., 2007).

Normal mixture modeling was used to identify the distribution of log-transformed PIB DVR data in the clinically normal participants (Mormino et al., 2014b, http://cran.r-project.org/web/packages/mclust/index.html). The data were best described by 2 distributions, and subjects were classified as having low or high amyloid burden for further analyses (low amyloid burden: N = 79, DVR range = 0.96–1.21; high amyloid burden: N = 29, DVR range = 1.29–1.73).

2.3. Diffusion tensor imaging

DTI images were acquired with a standard DTI sequence with 30 diffusion encoding gradient directions (repetition time [TR] = 8040 ms, echo time [TE] = 84 ms, inversion time [TI] = 2100 ms, 2 × 2 × 2 mm voxels, 64 transverse slices, b-value = 700 s/mm^2). Because of upgrades to the scanner used at baseline that took place subsequent to the baseline data collection, MR images at baseline and follow-up were acquired on 2 different but matched scanners at the Athinoula A. Martinos Center for Biomedical Imaging (Boston, USA). The 2 scanners were matched 3T Trio Tim scanners (Siemens Medical Systems, Erlangen, Germany) with 12-channel phased-array head coils and peak gradient strengths of 40 mT/m. For 12 young adults (20–30 years) who were scanned on both scanners within a period of less than 8 weeks, the FreeSurfer estimates of whole brain volume (WBV) obtained from a T1-weighted scan from both scanners were almost identical (mean scanner 1 = 1926.9 cm^3; mean scanner 2 = 1927.3 cm^3; t = −0.001, $p = 0.99$; r > 0.99), suggesting that the change in scanner had no notable effect on volumetric estimates. For our study sample of 108 older adults scanned over several years, the correlation between measurements of ROI FA (r > 0.82), mean diffusivity (MD; r > 0.85), radial diffusivity (r > 0.89), axial diffusivity (r > 0.76), WMH volumes (r = 0.96), WBV (r = 0.99), and hippocampus volumes (r = 0.97) was also high.

Processing of DTI data was performed in FSL (The Oxford Centre for Functional MRI of the Brain Software Library) v5.0.1 and closely follows current methods for processing of longitudinal DTI data in aging (Ito et al., 2015; Lövdén et al., 2014; Sexton et al., 2014). A schematic overview of the processing steps is shown in Fig. 1.

First, diffusion images were corrected for eddy current distortions and simple head motion by affine registration to the first B0 volume. During this step, the root-mean-square difference (in mm) of the 3 rotation and 3 translation parameters was calculated for each volume relative to the preceding volume and averaged over all volumes of the scan as a summary measure of head motion. Notably, individuals with low amyloid burden moved their head, on average, 0.08 mm (standard deviation [SD] = 0.52) less at the second scan than the first scan, whereas individuals with high amyloid burden moved, on average, 0.05 mm (SD = 0.37) more at the second scan. The time-dependent change in head motion resulted in a slight difference in head motion at follow-up for individuals with low amyloid burden (mean motion = 0.77 mm, SD = 0.37; t (104) = −2.17, $p = 0.03$) compared to individuals with high amyloid burden (mean motion = 0.95 mm, SD = 0.39), which was considered in subsequent analyses.

Next, images were skull stripped using FSL's brain extraction tool (Smith, 2002), and the diffusion tensor model was fitted at each voxel to describe the rate of diffusion along the main axis (axial diffusivity), perpendicular to the main axis (radial diffusivity, computed as the average of the 2 minor axes), as MD (the average rate of diffusion along all 3 axes) and as FA, which is also computed from all 3 axes to describe the directionality of diffusion in the voxel. FA takes a scalar value between 0 and 1 where 0 denotes equal diffusivity along all 3 axes, and a higher value indicates constrained diffusion in 1 direction.

All FA images were registered to a common space (the FMRIB58 FA image, a 1 × 1 × 1 mm FA MNI152 standard-space image), using FSLs FNIRT nonlinear registration with configurations optimized for FA data (they can be viewed in the T1_2_MNI152_2 mm configuration file distributed with FSL). The normalization parameters derived from the FA images were applied to the axial and radial diffusion images. Next, mean FA and diffusivity measures for each subject at each time point was computed for 12 ROIs that are defined using the John Hopkins University ICBM-DTI-81 white matter labels atlas (Mori et al., 2008; Fig. 1). ROIs were selected consistent with a previous study that has investigated the cross-sectional association between amyloid burden and FA (Chao et al., 2013) to include the major association fibers (superior longitudinal fasciculus, superior frontal occipital fasciculus, inferior frontal occipital fasciculus), projection fibers (anterior, superior, and posterior corona radiata and internal capsule), corpus callosum (genu, body, and splenium), and limbic fibers (cingulum and parahippocampal cingulum). The locations and trajectories of these structures in the human brain are described in detail in Wakana et al. (2004). Note, although the fornix has received considerable attention in aging and AD, it was not included in the current analyses because of its close proximity to cerebrospinal fluid and thus high sensitivity to partial volume effects. Pertaining to this point, individual baseline FA values in all included ROIs exceeded 0.2 at baseline and follow-up, whereas FA values below 0.2 were observed in fornix for 14% of the participants at baseline and 18% at follow-up. FA values below 0.2 are unlikely to be white matter and probably contaminated by cerebrospinal fluid (Smith et al., 2006).

Because the nonlinear warp to standard space is imperfect, in a secondary analysis, an additional preprocessing step was added to the DTI processing where the normalized FA images from all individuals at both time points were averaged to create a sample-specific white matter skeleton (thresholded at mean FA > 0.2; Smith et al., 2006). Each subject's aligned FA image was projected to the skeleton by searching perpendicular to the local skeleton for the maximum values in each individual FA image. This step is included to account for residual misalignments between individuals after the initial nonlinear registrations. However, because this procedure relies on the average FA image of a given sample, this also means that ROIs are sample specific.

2.4. Brain volumetrics

The T1-weighted multiecho magnetisation-prepared rapid gradient-echo scan (TR = 2200 ms, TI = 1100 ms, image1 TE = 1.54 ms, image2 TE = 3.36 ms, image3 TE = 5.18 ms, image4 TE = 7.01 ms, 1.20 mm isotropic voxel size) was used to estimate WBV, total intracranial volume (eTIV; Buckner et al., 2004), and bilateral hippocampal volume for each subject at each time point. To extract these estimates, images were processed with the longitudinal stream in FreeSurfer v 5.1.0 (Reuter and Fischl, 2011; Reuter et al., 2011, 2012). WBV at baseline was adjusted for each subject by using the following formula: adjusted WBV

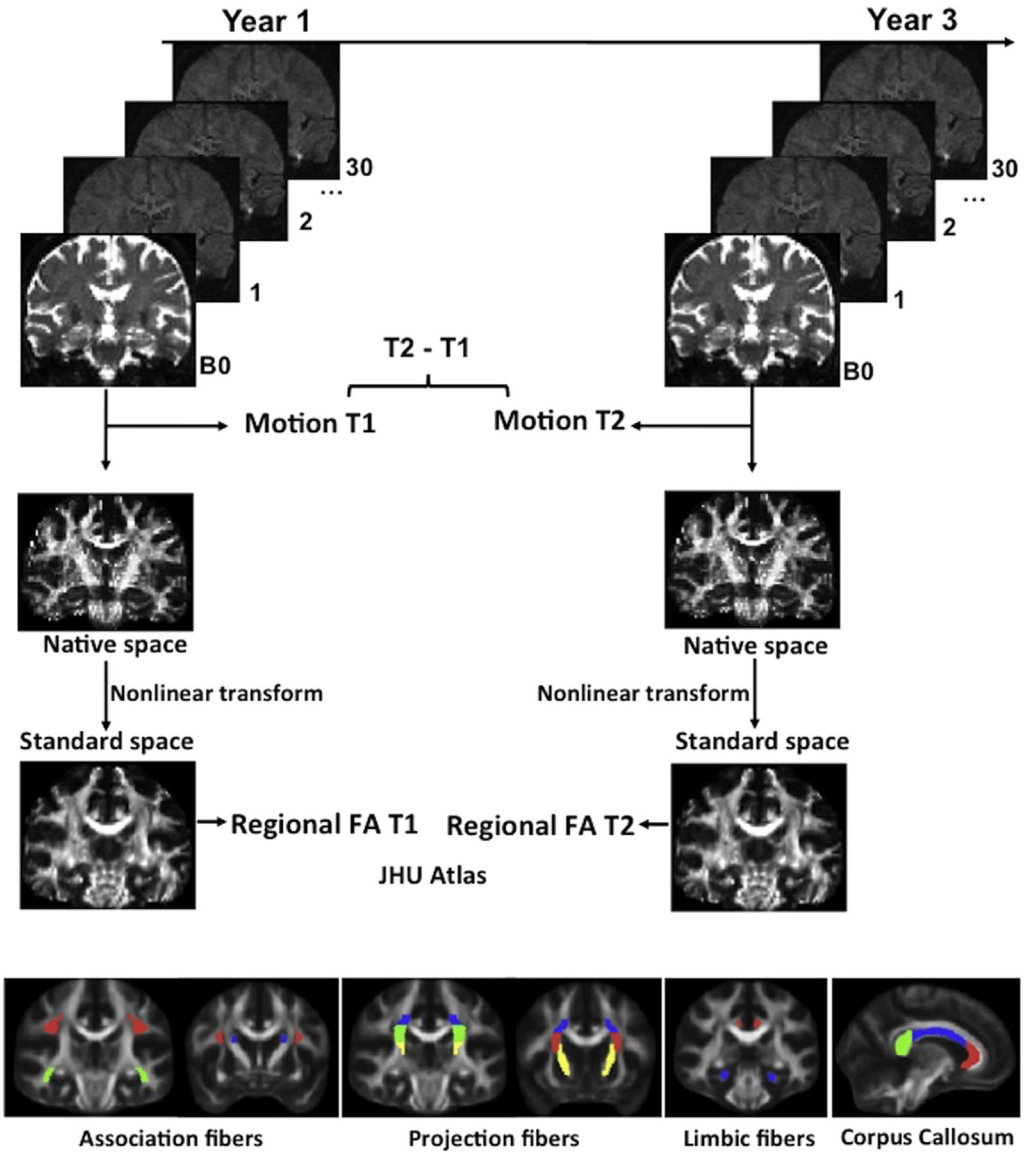

Fig. 1. Data processing. DTI data for each subject were processed independently at each time point. DTI scans were preprocessed to generate fractional anisotropy (FA) maps, motion (average rotation and translation parameters) estimates were saved and included in the longitudinal analyses as a time-dependent covariate. FA images were transformed to standard space to compute mean FA in 12 atlas-based regions of interest at each time point: major association fibers (red = superior longitudinal fasciculus, blue = superior frontal occipital fasciculus, and green = inferior frontal occipital fasciculus), projection fibers (red = anterior, blue = superior, green = posterior corona radiate, and yellow = internal capsule), corpus callosum (red = genu, blue = body, and red = splenium), and limbic fibers (red = cingulum and blue = parahippocampal cingulum). (For interpretation of the references to color in this figure legend, the reader is referred to the Web version of this article.)

(aWBV) = WBV − *b*(eTIV − mean eTIV), with mean eTIV reflecting the mean eTIV of the sample and b the regression coefficient for WBV against eTIV (see Buckner et al., 2004 for discussion). The same procedure was used to adjust hippocampal volumes. Where longitudinal change in volumes was of interest, volumes were adjusted across both scans.

2.5. White matter hyperintensities

A fluid-attenuated inversion recovery scan (TR = 6000 ms, TE = 454 ms, 1.0 × 1.0 × 1.5 mm voxels) obtained at each time point was used to compute WMH. WMH were calculated on skull-stripped (Smith, 2002) images using methods previously described (Wu et al., 2006). Initiating WMH seed regions were identified based on the intensity histogram of the image and iteratively updated. From the resulting WMH segmentation, the total WMH volume in mm^3 was estimated within a mask defined by the Johns Hopkins University White Matter Atlas, which was reverse normalized to the native space of each individual's fluid-attenuated inversion recovery scan image.

2.6. Linear mixed-effects models

Longitudinal change in DTI metrics (FA, mean, radial, and axial diffusivity) was explored in linear mixed-effects models, which contained a fixed effect for time (number of years between baseline and follow-up), baseline age as a covariate and a random intercept for each subject. The first model estimated mean annual change for each DTI metric in each ROI, controlling for baseline age only. For comparison, cross-sectional linear regression models were used to estimate the association between age and DTI metrics in the baseline data (Supplement 1).

The main analysis investigated a model including the interactions of amyloid burden with time and the interaction of APOE4 status with time as the predictors of interest. To estimate whether effects in a given tract are specific to the tract or reflect in part the general brain white matter integrity, FA (MD, radial, or axial diffusivity depending on the outcome variable) across all ROIs, and its interaction with time was also included in the model. This was motivated by prior reports which indicate that cross-sectional and longitudinal FA data across multiple tracts are best described by including both specific factors for individual tracts across hemispheres and a general factor capturing between-person differences in whole brain FA (Lövdén et al., 2013, 2014; Penke et al., 2010). Similarly, aWBV at baseline and its interaction with time were included as predictors in the model to estimate whether effects of amyloid burden on white matter integrity can be observed independent of individual differences in global atrophy. Baseline age, sex, head motion, and change in head motion over time were entered as covariates of no interest. The significance level for these analyses was adjusted to 0.004 which corresponds to a Bonferroni correction of $p = 0.05$ (1-tailed) for 12 ROIs.

Informed by significant findings in the first set of analyses, follow-up analyses were focused on the parahippocampal cingulum only. First, the models relating amyloid burden at baseline to change in white matter integrity were repeated after excluding participants that showed a change in CDR over time, to determine whether these individuals drive the observed associations. In the next set of follow-up analyses, decline in hippocampal volume over time was estimated using linear mixed-effects models with interactions of amyloid burden with time and the interaction of APOE4 status with time as effects of interest and covariates for baseline age and sex and their interactions with time. Then, to investigate whether hippocampal volume reduction and amyloid burden have synergistic effects on parahippocampal white matter integrity, linear mixed-effect models for FA in the parahippocampal cingulum were estimated (1) with inclusion of an amyloid burden × time interaction and a baseline hippocampal volume × time interaction and (2) with inclusion of an amyloid burden × time interaction, a baseline hippocampal volume × time interaction, and their joint interaction with time. These analyses were also performed with a time-dependent variable for hippocampal volume change over time, which examines whether hippocampal volumes change contributes to FA change in addition to hippocampus volume at baseline. In keeping with the main analyses, this model also included terms for APOE4 status, aWBV, average FA across ROIs and their interactions with time, as well as covariates for baseline age, sex, head motion at baseline (plus interactions with time), and change in head motion over time.

In a separate analysis, we estimated annual change in WMH volume, and explored WMHs as a covariate in the analyses linking elevated amyloid burden and FA to account for microstructural changes that are primarily driven by overt lesions.

Effects of amyloid burden and APOE4 status on parahippocampal white matter integrity were estimated separately for mean, axial, and radial diffusivity, following the same analysis as described for FA.

For all analyses, predictor variables and covariates were transformed in the following way to generate meaningful intercepts at 0 and units of 1: amyloid burden was coded as 1 (high amyloid) and 0 (low amyloid), APOE4 status was coded as 1 (e4+) and 0 (e4−), females and males as 0 and 1, respectively. Age was set at 0 for the sample minimum age (66) and an increase of 1 for each additional year. aWBV, mean FA across all ROIs (mean, axial, or radial diffusivity), and hippocampal volume at baseline were scaled to a sample mean of 0 and SD of 1. Time-dependent change in hippocampal volume was set as 0 at baseline, and the percent change from scan 1 to scan 2 at follow-up. Head motion was included as a covariate both as a baseline measure (scaled to a sample mean of 0 and SD of 1) and as a time-dependent covariate, which measures the difference in motion estimates between the 2 time points (i.e., a value of 1 indicates an increase in motion at follow-up by 1 mm).

Linear mixed-effects models were fitted in R with lme4 (Bates et al., 2015) using restricted maximum likelihood estimation and degrees of freedom for fixed effects were estimated by Satterthwaite approximation as implemented in lmerTest (http://cran.r-project.org/web/packages/lmerTest/index.html).

3. Results

3.1. White matter integrity declines over time

Average within-person mean annual changes are plotted and reported in Fig. 2 for FA in each region. FA significantly ($p < 0.05$, corrected for 12 comparisons) declined over time in association fibers (inferior frontal occipital fasciculus, superior frontal occipital fasciculus, superior longitudinal fasciculus; Fig. 2 row 1), projection fibers (superior and posterior corona radiata and internal capsule; Fig. 2 row 2), limbic fibers (cingulum and parahippocampal cingulum), and the body of corpus callosum (Fig. 2 row 3). Mean annual change in FA across significant regions was 0.5%. A significant increase in MD (a composite of axial and radial diffusivity) was found in association fibers (inferior frontal occipital fasciculus, superior frontal occipital fasciculus, superior longitudinal fasciculus; Table 1). Inspecting axial and radial diffusivity revealed significant increases in inferior and superior frontal occipital fasciculus; for the superior longitudinal fasciculus, only increases in radial diffusivity were significant. Also comparable to the pattern of changes observed for FA, projection fibers (superior and posterior corona radiata), limbic fibers (cingulum and parahippocampal cingulum), and the body of corpus callosum showed significant increases in MD (Table 1). Changes in diffusivity in the cingulum bundle and the body of the corpus callosum were driven by significant increases in radial diffusivity only; all other regions showed significant increases in axial and radial diffusivity. Unlike the changes in FA, no significant increases in diffusivity were observed for the internal capsule. Notably, within-person changes in FA, MD, as well as radial and axial diffusivity separately, did not meet the significance threshold in the splenium and genu after controlling for multiple comparisons (FA: $p = 0.005$ and $p = 0.02$, uncorrected; diffusivity measures <0.05, uncorrected; Table 1, Fig. 2) and did not meet the uncorrected threshold for the anterior corona radiata (FA and all diffusivity measures $p > 0.05$; uncorrected; Table 1, Fig. 2).

For comparison, Fig. 2 and Supplement 1 also report average cross-sectional age differences in FA and diffusivity measures in this sample, estimated in the baseline data. Global WMH volume also increased significantly over time with annual change estimated at 0.88% (estimate = 0.063, standard error [SE] = 0.001, $p < 0.001$, controlling for baseline age; cross-sectional annual change = 0.87%; estimate = 0.061, SE = 0.014, $p < 0.001$).

3.2. Amyloid burden at baseline predicts subsequent decline in parahippocampal white matter integrity

Significantly steeper decline in FA for individuals with amyloid burden at baseline compared to those without measurable amyloid burden was found in 1 of the 12 examined regions, the parahippocampal cingulum (estimate = −0.0046, SE = 0.0017, $p = 0.003$). Adopting the same model as described for FA for MD, radial, and axial diffusivity showed that amyloid burden in the parahippocampal cingulum was also weakly related to increasing MD,

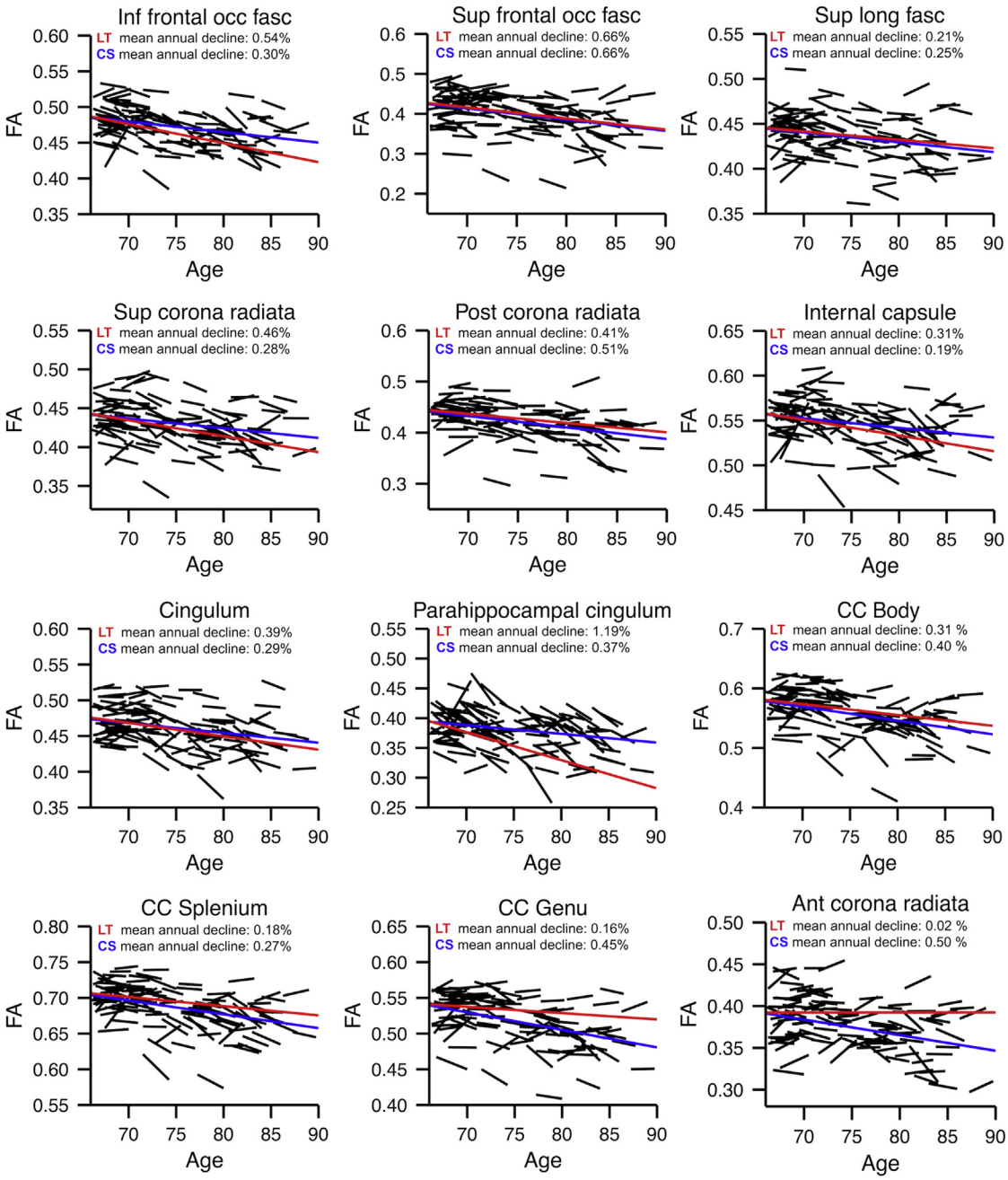

Fig. 2. Aging-related changes in FA. Raw FA data are plotted in black lines for each individual for 12 regions of interest. Beta estimates for average annual longitudinal (LT) change are plotted in solid red lines from a linear mixed model. Estimates of cross-sectional (CS) associations with age, estimated in baseline data only, are plotted in blue. The plotted effects are estimated after controlling for baseline age. The only estimates that are not significant at $p < 0.05$ (Bonferroni-corrected) are the longitudinal estimates for splenium, genu, and anterior corona radiata (bottom row). Abbreviation: FA, fractional anisotropy. (For interpretation of the references to color in this figure legend, the reader is referred to the Web version of this article.)

although it did not reach the adjusted significance criterion here (estimate = 0.008; SE = 0.004, $p = 0.02$, uncorrected). Radial diffusivity (estimate = 0.009, SE = 0.004, $p = 0.006$) but not axial diffusivity (estimate = 0.0006, SE = 0.0005, $p = 0.13$) showed a significantly steeper increase with high amyloid burden at baseline. After exclusion of 12 participants who showed a change in CDR over time (from 0 to 0.5), the associations between amyloid burden at baseline and change in FA (estimate = −0.0057, SE = 0.0018, $p = 0.002$), MD (estimate = 0.011, SE = 0.004, $p = 0.01$), radial (estimate = 0.012, SE = 0.004, $p = 0.002$), and axial diffusivity (estimate = 0.0008, SE = 0.005, $p = 0.06$) remained, indicating that the observed associations are not driven by these individuals. A cross-sectional analysis in this sample with the same set of predictors showed no significant effect of either amyloid burden or APOE4 status on FA or any of the diffusivity measures in this region (p values > 0.20; Supplement 2 reports cross-sectional results for the entire baseline sample N = 247). Fig. 3A re-plots the raw data shown for the parahippocampal cingulum in Fig. 2 separated by individuals with and without measurable amyloid burden. Fig. 3B shows the estimates from the interaction between amyloid burden (high = Aβ+, low = Aβ−) and time from the full linear mixed-effects model including amyloid status and APOE4, average FA

Table 1
Aging-related change in diffusivity

Region of Interest	Mean diffusivity		Axial diffusivity		Radial diffusivity	
	Intercept	% Annual increase	Intercept	% Annual increase	Intercept	% Annual increase
Inferior frontal occipital fasciculus	0.974	0.71[a]	1.498	0.34[a]	0.711	1.10[a]
Superior frontal occipital fasciculus	0.807	0.70[a]	1.184	0.31[b]	0.664	1.07[a]
Superior longitudinal fasciculus	0.784	0.25[a]	1.185	0.07	0.583	0.44[a]
Anterior corona radiata	0.661	−0.02	1.211	0.04	0.661	−0.08
Superior corona radiata	0.777	0.56[a]	1.168	0.38[a]	0.581	0.75[a]
Posterior corona radiata	0.884	0.60[a]	1.325	0.37[a]	0.663	0.84[a]
Internal capsule	0.744	0.15	1.266	−0.03	0.483	0.39[b]
Cingulum	0.768	0.26[a]	1.203	0.04	0.548	0.50[a]
Parahippocampal cingulum	0.904	1.50[a]	1.255	0.93[a]	0.729	1.99[a]
Genu	1.122	−0.04	1.755	−0.10	0.805	0.02
Body	0.970	0.31[a]	1.661	0.04	0.624	0.65[a]
Splenium	0.853	−0.02	1.689	−0.20	0.435	0.23

Intercept denotes the estimated diffusivity (×1000) for a 66-year-old individual (the minimum age in this sample) at baseline.
[a] Significant decline at Bonferroni-corrected level ($p < 0.004$).
[b] Significant at conventional level $p < 0.05$, +.

across ROIs and aWBV (plus interactions with time), as well as covariates for age, sex, baseline head motion (plus interactions with time), and change in head motion over time. Of note, in a simple longitudinal model including only amyloid status, APOE4 status, and the covariates age, sex, and head motion (plus interactions with time), the interaction between time and amyloid remained significant at conventional significance level, but the estimate of the interaction was slightly lower (estimate = −0.0036, SE = 0.0017, $p = 0.02$), suggesting that including predictors of whole brain integrity (i.e., aWBV and average FA across all ROIs) in the main analysis helped the identification of the tract-specific effect of amyloid in the parahippocampal cingulum. To investigate confounding effects of imperfect registration to standard space, FA in the parahippocampal gyrus was also estimated in the sample-specific skeletonized ROI, which included an additional preprocessing step that attempts to account for residual misalignment. The amyloid × time interaction was still present (estimate = −0.0112; SE = 0.0041, $p = 0.004$) for these FA estimates.

In addition to changes in white matter integrity of the parahippocampal cingulum, weak effects (i.e., not surviving the correction for multiple comparisons) of amyloid burden on increases in diffusivity over time were noted in the body of corpus callosum (MD: estimate = 0.0062, SE = 0.0024, $p = 0.005$; axial: estimate = 0.0088, SE = 0.0033, $p = 0.004$; radial: estimate = 0.0047, SE = 0.02, $p = 0.02$), anterior corona radiata (MD: estimate = 0.0034, SE = 0.0021, $p = 0.05$; axial: estimate = 0.0035, SE = 0.0020, $p = 0.05$; radial: estimate = 0.0035, SE = 0.0022, $p = 0.06$), and superior frontal occipital fasciculus (MD: estimate = 0.0065, SE = 0.0035, $p = 0.03$; axial: estimate = 0.0071, SE = 0.0039, $p = 0.04$; radial: estimate = 0.0063, SE = 0.0035, $p = 0.04$). There was no significant interaction between APOE4 and time in any ROI for any of the models and outcome variables (p values > 0.20).

Increase in WMH volume over time was not predicted by baseline amyloid burden. In addition, neither self-reported hypertension (yes/no) nor change in WMH over time had notable effects on the association between amyloid burden at baseline and decline in parahippocampal cingulum FA over time. Further post hoc analyses exploring the significant relation between amyloid burden at baseline and longitudinal decline in FA in the parahippocampal cingulum that emerged from the initial set of analyses are reported next.

3.3. *Associations between amyloid burden and loss of parahippocampal white matter integrity are independent of neurodegeneration*

First, we examined possible synergistic effects of baseline hippocampal atrophy and amyloid burden on parahippocampal white matter decline to establish whether high amyloid in normals is associated with parahippocampal cingulum FA, above and beyond hippocampal atrophy. Fig. 4A shows the data for hippocampal volume, separated by individuals with high and low amyloid burden.

For individuals with high amyloid burden at baseline, average longitudinal decline in hippocampal volume was estimated at 108 mm^3/y (=1.5%; controlling for baseline age). For individuals with low amyloid at baseline, the estimate was 49 mm^3/y (=0.6%;

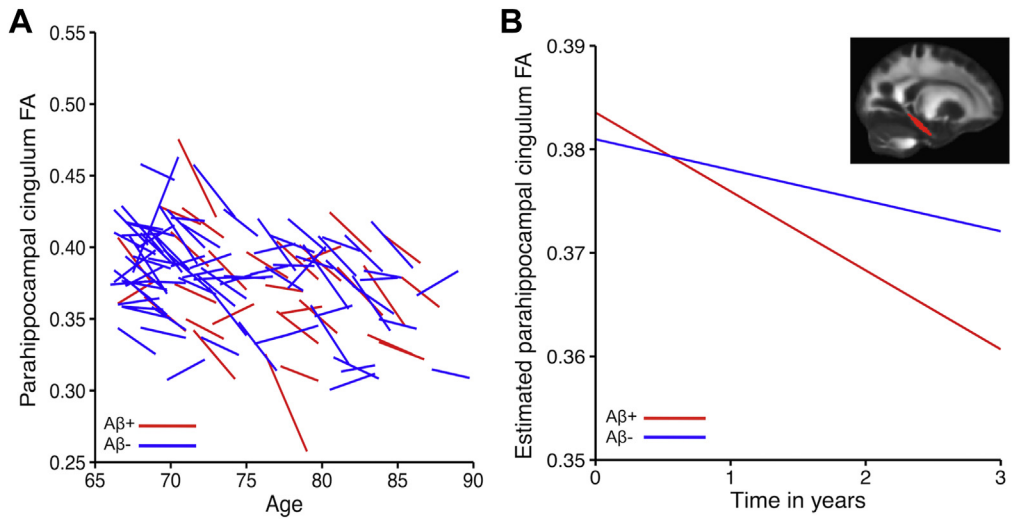

Fig. 3. Association between amyloid burden and change in FA. Within-person trajectories of change for parahippocampal cingulum FA (A) and average estimates of annual decline for individuals with and without measurable amyloid burden at baseline (B) are shown. Abbreviation: FA, fractional anisotropy.

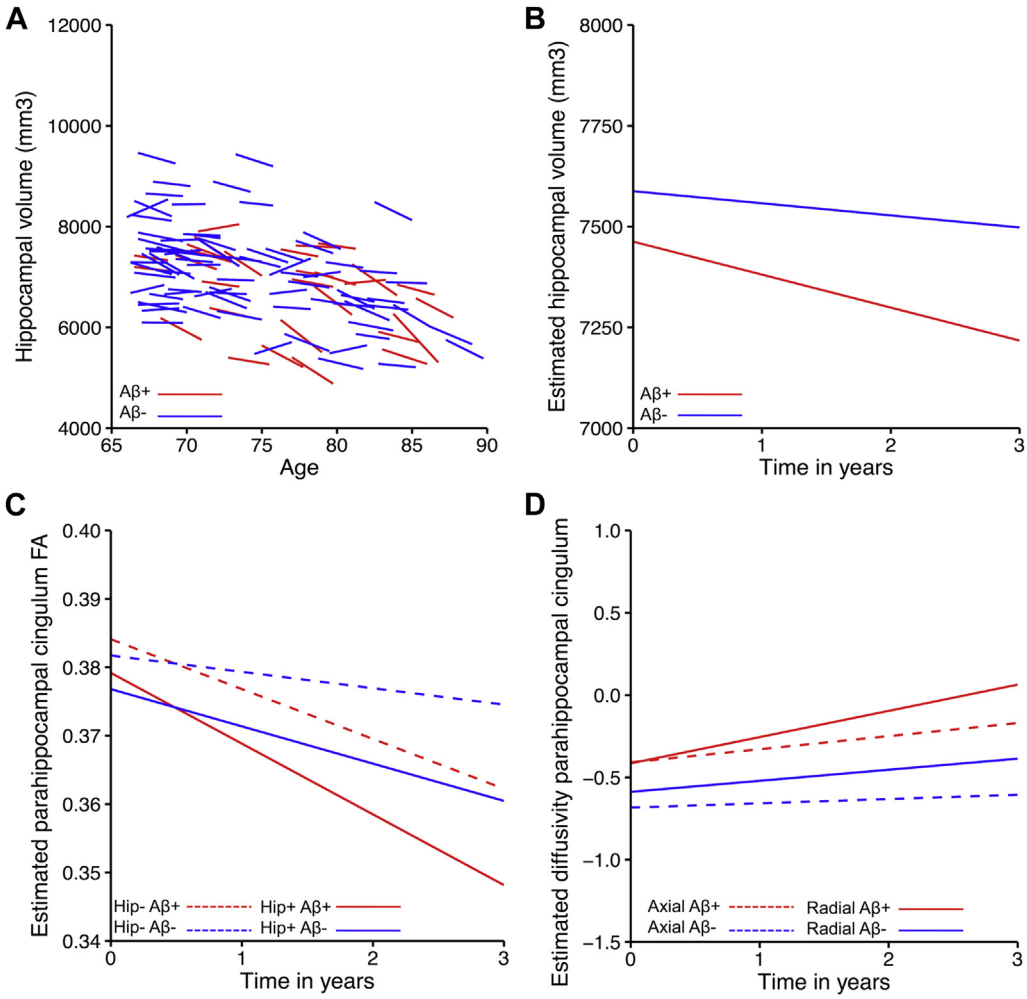

Fig. 4. Associations between amyloid burden and parahippocampal white matter integrity are independent of hippocampus volume. Plots shows within-person trajectories of change for hippocampal volume (A) and average estimates of annual decline for individuals with (Aβ+) and without (Aβ−) measurable amyloid burden (B). The effect of amyloid burden at baseline on FA decline in the parahippocampal cingulum bundle, independent of hippocampal atrophy, is shown in (C) Significant increases for Aβ+ versus Aβ− are observed for radial diffusivity (solid lines) but not axial diffusivity (dashed lines). For illustration purposes, hippocampal atrophy was re-coded as low atrophy (Hip−, i.e., larger hippocampi) and high atrophy (Hip+, i.e., smaller hippocampi) by median split. Radial and axial diffusivity were z-transformed. Beta estimates from linear mixed models are shown for graphs in panels B–D.

controlling for baseline age). The interaction between amyloid burden and time was significant for hippocampal volume in this sample (estimate = −51.83, SE = 15.70, $p = 0.001$, controlling for baseline age and the interaction between baseline age and time (Fig. 4B); estimate = −47.58, SE = 17.00, $p = 0.006$, controlling for age, sex, and APOE4 status and their interactions with time). The interaction between amyloid burden and time for WBV change over time was significant only at trend level (estimate = −1.63; SE = 0.94, $p = 0.09$; controlling for age, sex, and APOE4 status and their interactions with time).

When hippocampal volume and amyloid burden at baseline were entered as joint predictors of longitudinal decline in parahippocampal cingulum FA, the effect of amyloid on FA decline remained significant (estimate = −0.0045, SE = 0.0016, $p = 0.004$). Hippocampal volume at baseline was not associated with accelerated loss of white matter integrity in the parahippocampal cingulum (estimate = −0.0011, SE = 0.0009, $p = 0.25$), and there was no interaction between amyloid burden and hippocampus volume at baseline ($p = 0.75$), suggesting that the effect of baseline amyloid burden on parahippocampal cingulum FA is independent of baseline hippocampus volume (again controlling for APOE4 status, age, sex, motion, average FA across ROIs and aWBV, plus their interactions with time). To illustrate the independent effect of amyloid burden on subsequent change in white matter integrity (Fig. 4C), the sample was divided into those with more (Hip+) or less (Hip−) hippocampal atrophy using a median split (median volume = 7098.79 mm^3). Adding a term for hippocampal volume change over time to the model did not influence the interaction of baseline amyloid burden with time on FA and showed no significant relation with change in parahippocampal cingulum FA ($p = 0.59$).

The relations between amyloid burden and changes in diffusivity (Fig. 4D) were also still observed even after accounting for hippocampal volume at baseline, which in itself was associated with changes in both radial and axial diffusivity at trend level such that smaller hippocampi at baseline were associated with subsequent increases in radial diffusivity (estimate: −0.0038, SE = 0.0022, $p = 0.08$) and axial diffusivity (estimate: −0.0005, SE = 0.0003, $p = 0.08$).

4. Discussion

Reduced white matter integrity measured with DTI is a common finding in patients with AD, yet cross-sectional studies in clinically normal older individuals show mixed evidence for a reliable

association between markers of AD risk and white matter microstructure. The present study finds accelerated decline in FA and increase in radial diffusivity in the parahippocampal cingulum over a period of 2.6 years for individuals with elevated amyloid burden at baseline. Interestingly, no association between amyloid burden and FA or radial diffusivity was observed at baseline in this region, suggesting that loss of white matter integrity associated with elevated amyloid burden might become apparent only when following individuals over time. Diverging longitudinal and cross-sectional effects have also been reported for the association of amyloid burden with behavioral outcomes, gray matter atrophy and glucose metabolism (Knopman et al., 2013; Landau et al., 2012; Mattsson et al., 2014; Storandt et al., 2009). This indicates more generally that samples of clinically normal individuals are likely not homogeneous and that longitudinal analyses are of particular importance when behavior and biomarkers are investigated in relation to amyloid burden.

While significant longitudinal change in white matter integrity was found across almost all regions, a reliable association between amyloid burden and change in white matter microstructure was selective for the parahippocampal cingulum. Trends for an association of amyloid burden with steeper increases in diffusivity only were also observed in body of the corpus callosum, anterior corona radiata, and superior frontal occipital fasciculus. This suggests that diffusivity estimates may be able to pick up subtle changes in white matter integrity that remain undetected by FA, consistent with prior reports in healthy individuals (Westlye et al., 2012) and AD (Salat et al., 2010). However, given the low statistical significance for amyloid-related increases in diffusivity (i.e., not surviving multiple comparisons), this particular finding must be interpreted cautiously. In the following paragraphs, the role of the parahippocampal gyrus in aging and AD, longitudinal versus cross-sectional examinations of white matter integrity, and some limitations of the present study are discussed in more detail.

4.1. The parahippocampal cingulum in aging and AD

The cingulum bundle collectively describes the short and long association fibers of the cingulate gyrus that run parallel to the corpus callosum between genu and splenium. At the retrosplenial cortex, white matter fibers of the cingulum connect to the temporal lobe and terminate in the cortex of the parahippocampal gyrus and subiculum (Jones et al., 2013; Mufson and Pandya, 1984). Because the parahippocampal portion of the cingulum bundle provides one important pathway through which the hippocampal complex is connected with cortical areas, it has been the focus of many studies in AD.

Zhang et al. (2007) demonstrated reduced white matter integrity as measured with DTI in the parahippocampal cingulum in patients with AD. They also showed that, while altered DTI measures in AD extended to the splenium, reduced FA in mild cognitive impairment was confined to the parahippocampal and posterior portions of the cingulum. This suggests that DTI measures might be sensitive to the progression of AD pathology from the hippocampal complex to posterior association cortices. In line with this interpretation, in the current sample of clinically normal older adults, accelerated loss of white matter integrity for clinically normal individuals that are at an increased risk for Alzheimer's dementia was found in the parahippocampal white matter. It is possible that with longer follow-up periods, we would begin to see preclinical white matter changes also in posterior portions of the cingulum and parietal areas, both in terms of microstructural indices and WMH, in individuals that are on the path to AD.

The initial findings in AD from Zhang et al. (2007) were confirmed in a whole brain analysis by Salat et al. (2010). Consistent with histopathological studies, both studies showed that reduced FA in the parahippocampal cingulum bundle was statistically independent of hippocampal neurodegeneration and speculate that reduced FA may primarily reflect demyelination. Animal studies have linked increases in radial diffusivity to demyelination and decreases in axial diffusivity to axonal damage (Budde et al., 2007; Song et al., 2002, 2003, 2005). In line with the interpretation of white matter damage in parahippocampal cingulum reflecting primarily demyelination, Salat et al. (2010) demonstrated stronger increases in radial diffusivity compared with axial diffusivity in the parahippocampal white matter of AD patients. Again, the findings in AD are mirrored in the present study in clinically normal older adults with measurable amyloid burden: amyloid deposition was associated with FA decline in parahippocampal white matter independent of hippocampus volume loss and was pronounced for radial diffusivity over axial diffusivity (Fig. 4C and D).

In summary, DTI-based measures of white matter microstructure appear sensitive to AD pathology with the earliest changes appearing in the parahippocampal white matter in clinically normal individuals at increased risk for AD (present study) and spreading from there also to posterior cingulum in mild cognitive impairment (Zhang et al., 2007) and finally posterior association cortex in AD (Salat et al., 2010; Zhang et al., 2007). Future longitudinal investigations are warranted that explore the link between parahippocampal white matter changes in aging and AD, and functional "disconnection" of the hippocampus from adjacent cortex and the posterior cingulate that has been described with functional MRI (e.g., Greicius et al., 2004; Salami et al., 2014; Song et al., 2015; Ward et al., 2013) and in terms of glucose hypometabolism of the cingulate and subgenual cortices (Villain et al., 2010).

Subtle associations between APOE4 genotype and FA in the parahippocampal white matter have been reported in 2 small-scale studies (Honea et al., 2009; Tsao et al., 2014), but larger samples (Nyberg and Salami, 2014; Westlye et al., 2012) and the present study have not replicated this association. This suggests that APOE4 genotype has no effect on FA decline that is independent of amyloid status. That said, it is possible that studies in even larger samples would reveal independent contributions of APOE4 and amyloid on FA, as has been demonstrated for cognitive decline (Mormino et al., 2014b).

4.2. Limitations

Although this study has provided new insights into the progression of white matter damage in clinically normal older individuals, DTI remains an indirect measure of white matter integrity, and we are unable to determine the type of white matter damage or the cellular mechanisms by which amyloid and FA are linked. Studies have shown that amyloid accumulation and white matter damage are related in patients with cerebral amyloid angiopathy, suggesting that reduced white matter integrity could be primarily a reflection of vascular amyloid accumulation (Olichney et al., 2000). However, transgenic mice with neuritic plaques show reduced FA and reduced radial diffusivity over time, mirroring the pattern of change in the present study (Song et al., 2004). Moreover, cerebral amyloid angiopathy is associated with the APOE4 genotype (Olichney et al., 2000), so the fact that we did not find an effect between APOE and white matter integrity makes it unlikely that the association between amyloid burden and white matter integrity is exclusively caused by vascular amyloid. New PET tracers with increased specificity, novel targets, and the development of high angular resolution diffusion imaging may aid future studies to explore the cellular basis of white matter damage in the path to AD in more detail. In particular, additional in vivo evaluation of tau tangle burden in the hippocampal complex will be important to establish whether the white matter changes we observed are driven by increases in local tangle burden.

Another limitation of this study is that it remains an open question how reduced FA in the parahippocampal cingulum fits into the set of relationships between amyloid burden, neurodegeneration, and cognitive decline (Mormino et al., 2014a). These questions require complex multivariate analyses that are currently hindered by insufficient sample sizes as the expected effect sizes are small (Hedden et al., 2013, 2016; Mormino et al., 2014a, b)

5. Conclusions

Studies in AD have identified white matter abnormalities in the parahippocampal cingulum. The present study shows that amyloid burden modifies the integrity of this pathway in clinically normal individuals. Although there was no detectable effect of amyloid burden on DTI measures at baseline, accelerated change in FA and radial diffusivity in the parahippocampal cingulum was observed in individuals with amyloid burden at baseline over a period of 2.6 years. This effect appeared independent of amyloid-related changes in hippocampal volume. The results indicate that change in white matter integrity in the hippocampal complex may be a biomarker to target in individuals at increased risk for AD and also highlight the value of longitudinal research in aging and AD. Future research is necessary to examine the mechanisms by which amyloid burden leads to white matter damage and how this cascade is related to clinical progression.

Disclosure statement

The authors report no conflicts of interest.

Acknowledgements

This work was supported by National Institute on Aging grants (P01 AG036694, P50 AG005134, R01 AG034556, R01 AG027435, and K01 AG040197), the Alzheimer's Association grant (ZEN-10-174210), and by the Howard Hughes Medical Institute. Anna Rieckmann is supported by a Marie Curie International Outgoing Fellowship from the European Commission. This research was carried out in part at the Athinoula A. Martinos Center for Biomedical Imaging at the Massachusetts General Hospital, using resources provided by the Center for Functional Neuroimaging Technologies, a P41 Biotechnology Resource Grant supported by the National Institute of Biomedical Imaging and Bioengineering (NIBIB), National Institutes of Health (P41 EB015896). This work also involved the use of instrumentation supported by the NIH Shared Instrumentation Grant Program and/or High-End Instrumentation Grant Program (specifically S10RR023401, S10RR019307, S10RR019254, and S10RR023043). The authors are grateful for the help of all research assistants involved in the Harvard Aging Brain study (http://www.martinos.org/harvardagingbrain/Acknowledgements.html). They thank Elizabeth Mormino, David Salat, and Christian Wachinger for helpful discussions and advise on statistical analyses.

Appendix A. Supplementary data

Supplementary data associated with this article can be found, in the online version at http://dx.doi.org/10.1016/j.neurobiolaging.2016.03.016.

References

Barrick, T.R., Charlton, R.A., Clark, C.A., Markus, H.S., 2010. White matter structural decline in normal ageing: a prospective longitudinal study using tract-based spatial statistics. Neuroimage 51, 565–577.

Bartzokis, G., Sultzer, D., Lu, P.H., Nuechterlein, K.H., Mintz, J., Cummings, J.L., 2004. Heterogeneous age-related breakdown of white matter structural integrity: implications for cortical "disconnection" in aging and Alzheimer's disease. Neurobiol. Aging 25, 843–851.

Bates, D., Mächler, M., Bolker, B., Walker, S., 2015. Fitting Linear Mixed-effects Models Using Lme4. J. Stat. Softw. 67, 1–48.

Bender, A.R., Raz, N., 2015. Normal-appearing cerebral white matter in healthy adults: mean change over 2 years and individual differences in change. Neurobiol. Aging 36, 1834–1848.

Bozzali, M., Falini, A., Franceschi, M., Cercignani, M., Zuffi, M., Scotti, G., Comi, G., Filippi, M., 2002. White matter damage in Alzheimer's disease assessed in vivo using diffusion tensor magnetic resonance imaging. J. Neurol. Neurosurg. Psychiatry 72, 742–746.

Brickman, A.M., 2013. Contemplating Alzheimer's disease and the contribution of white matter hyperintensities. Curr. Neurol. Neurosci. Rep. 13, 415.

Brickman, A.M., Provenzano, F.A., Muraskin, J., Manly, J.J., Blum, S., Apa, Z., Stern, Y., Brown, T.R., Luchsinger, J.A., Mayeux, R., 2012. Regional white matter hyperintensity volume, not hippocampal atrophy, predicts incident Alzheimer disease in the community. Arch. Neurol. 69, 1621–1627.

Brun, A., Englund, E., 1986. A white matter disorder in dementia of the Alzheimer type: a pathoanatomical study. Ann. Neurol. 19, 253–262.

Buckner, R.L., Head, D., Parker, J., Fotenos, A.F., Marcus, D., Morris, J.C., Snyder, A.Z., 2004. A unified approach for morphometric and functional data analysis in young, old, and demented adults using automated atlas-based head size normalization: reliability and validation against manual measurement of total intracranial volume. Neuroimage 23, 724–738.

Budde, M.D., Kim, J.H., Liang, H.-F., Schmidt, R.E., Russell, J.H., Cross, A.H., Song, S.K., 2007. Toward accurate diagnosis of white matter pathology using diffusion tensor imaging. Magn. Reson. Med. 57, 688–695.

Chao, L.L., DeCarli, C., Kriger, S., Truran, D., Zhang, Y., Laxamana, J., Villeneuve, S., Jagust, W.J., Sanossian, N., Mack, W.J., Chui, H.C., Weiner, M.W., 2013. Associations between white matter hyperintensities and β amyloid on integrity of projection, association, and limbic fiber tracts measured with diffusion tensor MRI. PLoS One 8, e65175.

Charlton, R.A., Schiavone, F., Barrick, T.R., Morris, R.G., Markus, H.S., 2010. Diffusion tensor imaging detects age related white matter change over a 2 year follow-up which is associated with working memory decline. J. Neurol. Neurosurg. Psychiatry 81, 13–19.

Corder, E., Saunders, A., Strittmatter, W., Schmechel, D., Gaskell, P., Small, G., Roses, A.D., Haines, J.L., Pericak-Vance, M.A., 1993. Gene dose of apolipoprotein E type 4 allele and the risk of Alzheimer's disease in late onset families. Science 261, 921–923.

Englund, E., Brun, A., Alling, C., 1988. White matter changes in dementia of Alzheimer's type. Brain 111, 1425–1439.

Gomperts, S.N., Rentz, D.M., Moran, E., Becker, J.A., Locascio, J.J., Klunk, W.E., Mathis, C.A., Elmaleh, D.R., Shoup, T., Fischman, A.J., Hyman, B.T., Growdon, J.H., Johnson, K.A., 2008. Imaging amyloid deposition in Lewy body diseases. Neurology 71, 903–910.

Greicius, M.D., Srivastava, G., Reiss, A.L., Menon, V., 2004. Default-mode network activity distinguishes Alzheimer's disease from healthy aging: evidence from functional MRI. Proc. Natl. Acad. Sci. U. S. A. 101, 4637–4642.

Han, X., M Holtzman, D., McKeel, D.W., Kelley, J., Morris, J.C., 2002. Substantial sulfatide deficiency and ceramide elevation in very early Alzheimer's disease: potential role in disease pathogenesis. J. Neurochem. 82, 809–818.

Head, D., Buckner, R.L., Shimony, J.S., Williams, L.E., Akbudak, E., Contouro, T.E., McAvoy, M., Morris, J.C., Snyder, A.Z., 2004. Differential vulnerability of anterior white matter in nondemented aging with minimal acceleration in dementia of the Alzheimer type: evidence from diffusion tensor imaging. Cereb. Cortex 14, 410–423.

Hedden, T., Mormino, E.C., Amariglio, R.E., Younger, A.P., Schultz, A.P., Becker, J.A., Buckner, R.L., Johnson, K.A., Sperling, R.A., Rentz, D.M., 2012. Cognitive profile of amyloid burden and white matter hyperintensities in cognitively normal older adults. J. Neurosci. 32, 16233–16242.

Hedden, T., Oh, H., Younger, A.P., Patel, T.A., 2013. Meta-analysis of amyloid-cognition relations in cognitively normal older adults. Neurology 80, 1341–1348.

Hedden, T., Schultz, A.P., Rieckmann, A., Mormino, E.C., Johnson, K.A., Sperling, R.A., Buckner, R.L., 2016. Multiple brain markers are linked to age-related variation in cognition. Cereb. Cortex 26, 1388–1400.

Hedden, T., Van Dijk, K.R.A., Becker, J.A., Mehta, A., Sperling, R.A., Johnson, K.A., Buckner, R.L., 2009. Disruption of functional connectivity in clinically normal older adults harboring amyloid burden. J. Neurosci. 29, 12686–12694.

Heise, V., Filiippini, N., Ebmeier, K.P., Mackay, C.E., 2011. The APOE ε4 allele modulates brain white matter integrity in healthy adults. Mol. Psychiatry 16, 908–916.

Honea, R.A., Vidoni, E., Harsha, A., Burns, J.M., 2009. Impact of APOE on the healthy aging brain: a voxel-based MRI and DTI study. J. Alzheimer Dis. 18, 553–564.

Hyman, B., Van Hoesen, G., Damasio, A., Barnes, C., 1984. Alzheimer's disease: cell-specific pathology isolates the hippocampal formation. Science 225, 1168–1170.

Ito, K., Sasaki, M., Takahashi, J., Uwano, I., Yamashita, F., Higuchi, S., Goodwin, J., Harada, T., Kudo, K., Terayama, Y., 2015. Detection of early changes in the parahippocamapl and posterior cingulum bundles during mild cognitive impairment by using high-resolution multi-parametric diffusion tensor imaging. Psychiatry Res. 231, 346–352.

Johnson, K.A., Gregas, M., Becker, J.A., Kinnecom, C., Salat, D.H., Moran, E.K., Smith, E.E., Rosand, J., Rentz, D.M., Klunk, W.E., Mathis, C.A., Price, J.C., Dekosky, S.T., Fischman, A.J., Greenberg, S.M., 2007. Imaging of amyloid burden and distribution in cerebral amyloid angiopathy. Ann. Neurol. 62, 229–234.

Jones, D.K., Christiansen, K.F., Chapman, R.J., Aggleton, J.P., 2013. Distinct subdivisions of the cingulum bundle revealed by diffusion MRI fibre tracking: implications for neuropsychological investigations. Neuropsychologia 51, 67–78.

Jovicich, J., Marizzoni, M., Bosch, B., Bartrés-Faz, D., Arnold, J., Benninghoff, J., Wiltfang, J., Roccatagliata, L., Picco, A., Nobili, F., Blin, O., Bombois, S., Lopes, R., Bordet, R., Chanoine, V., Ranjeva, J.P., Didic, M., Gros-Dagnac, H., Payoux, P., Zoccatelli, G., Alessandrini, F., Beltramello, A., Bargalló, N., Ferretti, A., Caulo, M., Aiello, M., Ragucci, M., Soricelli, A., Salvadori, N., Tarducci, R., Floridi, P., Tsolaki, M., Constantinidis, M., Drevelegas, A., Rossini, P.M., Marra, C., Otto, J., Reiss-Zimmermann, M., Hoffmann, K.T., Galluzzi, S., Frisoni, G.B.PharmaCog Consortium, 2014. Multisite longitudinal reliability of tract-based spatial statistics in diffusion tensor imaging of healthy elderly subjects. Neuroimage 101, 390–403.

Kantarci, K., Schwarz, C.G., Reid, R.I., Przybelski, S.A., Lesnick, T.G., Zuk, S.M., Senjem, M.L., Gunter, J.L., Lowe, V., Machulda, M.M., Knopman, D.S., Petersen, R.C., Jack, J.R., 2014. White matter integrity determined with diffusion tensor imaging in older adults without dementia: influence of amyloid load and neurodegeneration. JAMA Neurol. 71, 1547–1554.

Klunk, W.E., 2011. Amyloid imaging as a biomarker for cerebral beta-amyloidosis and risk prediction for Alzheimer dementia. Neurobiol. Aging 32, S20–S36.

Knopman, D.S., Jack, C.R., Wiste, H.J., Weigand, S.D., Vemuri, P., Lowe, V.J., Kantarci, K., Gunter, J.L., Senjem, M.L., Mielke, M.M., Roberts, R.O., Boeve, B.F., Petersen, R.C., 2013. Selective worsening of brain injury biomarker abnormalities in cognitively normal elderly persons with β-amyloidosis. JAMA Neurol. 70, 1030–1038.

Landau, S.M., Mintun, M.A., Joshi, A.D., Koeppe, R.A., Petersen, R.C., Aisen, P.S., Weiner, M.W., Jagust, W.J.For the Alzheimer's Disease Neuroimaging Initiative, 2012. Amyloid deposition, hypometabolism, and longitudinal cognitive decline. Ann. Neurol. 72, 578–586.

Logan, J., Fowler, J.S., Volkow, N.D., Wolf, A.P., Dewey, S.L., Schlyer, D.J., MacGregor, R.R., Hitzemann, R., Bendriem, B., Gatley, S.J., Christman, D.R., 1990. Graphical analysis of reversible radioligand binding from time-activity measurements applied to [N-11C-methyl]-(-)-cocaine PET studies in human subjects. J. Cereb. Blood Flow Metab. 10, 740–747.

Lövdén, M., Köhncke, Y., Laukka, E.J., Kalpouzos, G., Salami, A., Li, T.-Q., Fratiglioni, L., Bäckman, L., 2014. Changes in perceptual speed and white matter microstructure in the corticospinal tract are associated in very old age. Neuroimage 102, 520–530.

Lövdén, M., Laukka, E.J., Rieckmann, A., Kalpouzos, G., Li, T.-Q., Jonsson, T., Wahlund, L.O., Fratiglioni, L., Bäckman, L., 2013. The dimensionality of between-person differences in white matter microstructure in old age. Hum. Brain Mapp. 34, 1386–1398.

Marchant, N.L., Reed, B.R., DeCarli, C.S., Madison, C.M., Weiner, M.W., Chui, H.C., Jagust, W.J., 2012. Cerebrovascular disease, β-amyloid, and cognition in aging. Neurobiol. Aging 33, 1006.e25–1006.e36.

Mattsson, N., Insel, P.S., Nosheny, R., Tosun, D., Trojanowski, J.Q., Shaw, L.M., Jack, C.R., Donohue, M.C., Weiner, M.W.Alzheimer's Disease Neuroimaging Initiative, 2014. Emerging β-amyloid pathology and accelerated cortical atrophy. JAMA Neurol. 71, 725–734.

Medina, D., deToledo-Morrell, L., Urresta, F., Gabrieli, J.D.E., Moseley, M., Fleischman, D., Bennett, D.A., Leurgans, S., Turner, D.A., Stebbins, G.T., 2006. White matter changes in mild cognitive impairment and AD: a diffusion tensor imaging study. Neurobiol. Aging 27, 663–672.

Mori, S., Oishi, K., Jiang, H., Jiang, L., Li, X., Akhter, K., Hua, K., Faria, A.V., Mahmood, A., Woods, R., Toga, A.W., Pike, G.B., Neto, P.R., Evans, A., Zhang, J., Huang, H., Miller, M.I., van Zijl, P., Mazziotta, J., 2008. Stereotaxic white matter atlas based on diffusion tensor imaging in an ICBM template. Neuroimage 40, 570–582.

Mormino, E.C., Betensky, R.A., Hedden, T., Schultz, A.P., Amariglio, Rentz, D.M., Johnson, K.A., Sperling, R.A., 2014a. Synergistic effect of β-amyloid and neurodegeneration on cognitive decline in clinically normal individuals. JAMA Neurol. 71, 1379–1385.

Mormino, E.C., Betensky, R.A., Hedden, T., Schultz, A.P., Ward, A., Huijbers, W., Rentz, D.M., Johnson, K.A., Sperling, R.A.Alzheimer's Disease Neuroimaging InitiativeAustralian Imaging Biomarkers and Lifestyle Flagship Study of AgeingHarvard Aging Brain Study, 2014b. Amyloid and APOE ε4 interact to influence short-term decline in preclinical Alzheimer disease. Neurology 82, 1760–1767.

Mufson, E.J., Pandya, D.N., 1984. Some observations on the course and composition of the cingulum bundle in the rhesus monkey. J. Comp. Neurol. 225, 31–43.

Nyberg, L., Salami, A., 2014. The APOE ε4 allele in relation to brain white-matter microstructure in adulthood and aging. Scand. J. Psychol. 55, 263–267.

Olichney, J.M., Hansen, L.A., Lee, J.H., Hofstetter, C.R., Katzman, R., Thal, L.J., 2000. Relationship between severe amyloid angiopathy, apolipoprotein E genotype, and vascular lesions in Alzheimer's disease. Ann. N. Y. Acad. Sci. 903, 138–143.

Ossenkoppele, R., Jansen, W.J., Rabinovivi, D., Knol, D.K., van der Flier, M., van Berckel, B.N.M., Scheltens, P., Visser, P.J.and the Amyloid PET Study Group, 2015. Prevalence of amyloid PET positivity in dementia syndomes: a meta-analysis. JAMA 313, 1939–1950.

Penke, L., Munoz Maniega, S., Murray, C., Gow, A.J., Valdes Hernandez, M.C., Clayden, J.D., Starr, J.M., Wardlaw, J.M., Bastin, M.E., Deary, I.J., 2010. A general factor of brain white matter integrity predicts information processing speed in healthy older people. J. Neurosci. 30, 7569–7574.

Price, J.C., Klunk, W.E., Lopresti, B.J., Lu, X., Hoge, J.A., Ziolko, S.K., Holt, D.P., Meltzer, C.C., DeKosky, S.T., Mathis, C.A., 2005. Kinetic modeling of amyloid binding in humans using PET imaging and Pittsburgh Compound-B. J. Cereb. Blood Flow Metab. 25, 1528–1547.

Rabinovici, G.D., Jagust, W.J., 2009. Amyloid imaging in aging and dementia: testing the amyloid hypothesis in vivo. Behav. Neurol. 21, 117–128.

Racine, A.M., Adluru, N., Alexander, A.L., Christian, B.T., Okonkwo, O.C., Oh, J., Cleary, C.A., Birdsill, A., Hillmer, A.T., Murali, D., Barnhart, T.E., Gallagher, C.L., Carlsson, C.M., Rowley, H.A., Dowling, N.M., Asthana, S., Sager, M.A., Bendlin, B.B., Johnson, S.C., 2014. Associations between white matter microstructure and amyloid burden in preclinical Alzheimer's disease: a multimodal imaging investigation. Neuroimage Clin. 4, 604–614.

Reuter, M., Fischl, B., 2011. Avoiding asymmetry-induced bias in longitudinal image processing. Neuroimage 57, 19–21.

Reuter, M., Rosas, H.D., Fischl, B., 2011. Highly accurate inverse consistent registration: a robust approach. Neuroimage 53, 1181–1196.

Reuter, M., Schmansky, N.J., Rosas, H.D., Fischl, B., 2012. Within-subject template estimation for unbiased longitudinal image analysis. Neuroimage 61, 1402–1418.

Rose, S.E., Chen, F., Chalk, J.B., Zelaya, F.O., Strugnell, W.E., Benson, M., Semple, J., Doddrell, D.M., 2000. Loss of connectivity in Alzheimer's disease: an evaluation of white matter tract integrity with colour coded MR diffusion tensor imaging. J. Neurol. Neurosurg. Psychiatry 69, 528–530.

Rutten-Jacobs, L.C.A., de Leeuw, F.-E., Geurts-van Bon, L., Gordinou de Gouberville, M.C., Schepens-Franke, A.N., Dederen, P.J., Spliet, W.G.M., Wesseling, P., Kiliaan, A.J., 2011. White matter lesions are not related to β-Amyloid deposition in an autopsy-based study. Curr. Gerontol. Geriatr. Res. 2011, 1–5.

Salami, A., Pudas, S., Nyberg, L., 2014. Elevated hippocampal resting-state connectivity underlies deficient neurocognitive function in aging. Proc. Natl. Acad. Sci. U. S. A. 111, 17654–17659.

Salat, D.H., Tuch, D.S., van der Kouwe, A.J.W., Greve, D.N., Pappu, V., Lee, S.Y., Hevelone, N.D., Zaleta, A.K., Growdon, J.H., Corkin, S., Fischl, B., Rosas, H.D., 2010. White matter pathology isolates the hippocampal formation in Alzheimer's disease. Neurobiol. Aging 31, 244–256.

Scheltens, P., Barkhof, F., Leys, D., Wolters, E.C., Ravid, R., Kamphorst, W., 1995. Histopathologic correlates of white matter changes on MRI in Alzheimer's disease and normal aging. Neurology 45, 883–888.

Sexton, C.E., Walhovd, K.B., Storsve, A.B., Tamnes, C.K., Westlye, L.T., Johansen-Berg, H., Fjell, A.M., 2014. Accelerated changes in white matter microstructure during aging: a longitudinal diffusion tensor imaging study. J. Neurosci. 34, 15425–15436.

Smith, S.M., 2002. Fast robust automated brain extraction. Hum. Brain Mapp. 17, 143–155.

Smith, S.M., Jenkinson, M., Johansen-Berg, H., Rueckert, D., Nichols, T.E., Mackay, C.E., Watkins, K.E., Ciccarelli, O., Cader, M.Z., Matthews, P.M., Behrens, T.E., 2006. Tract-based spatial statistics: voxelwise analysis of multi-subject diffusion data. Neuroimage 31, 1487–1505.

Sojkova, J., Resnick, S.M., 2011. In vivo human amyloid imaging. Curr. Alzheimer Res. 8, 366–372.

Song, S.-K., Kim, J.H., Lin, S.-J., Brendza, R.P., Holtzman, D.M., 2004. Diffusion tensor imaging detects age-dependent white matter changes in a transgenic mouse model with amyloid deposition. Neurobiol. Dis. 15, 640–647.

Song, S.-K., Sun, S.-W., Ju, W.-K., Lin, S.-J., Cross, A.H., Neufeld, A.H., 2003. Diffusion tensor imaging detects and differentiates axon and myelin degeneration in mouse optic nerve after retinal ischemia. Neuroimage 20, 1714–1722.

Song, S.-K., Sun, S.-W., Ramsbottom, M.J., Chang, C., Russell, J., Cross, A.H., Armstrong, R.C., 2002. Dysmyelination revealed through MRI as increased radial (but unchanged axial) diffusion of water. Neuroimage 17, 1429–1436.

Song, S.-K., Yoshino, J., Le, T.Q., Lin, S.-J., Sun, S.-W., Cross, A.H., Armstrong, R.C., 2005. Demyelination increases radial diffusivity in corpus callosum of mouse brain. Neuroimage 26, 132–140.

Song, Z., Insel, P.S., Buckley, S., Yohannes, S., Mezher, A., Simonson, A., Wilkins, S., Tosun, D., Mueller, S., Kramer, J.H., Miller, B.L., Weiner, M.W., 2015. Brain amyloid-β burden is associated with disruption of intrinsic functional connectivity within the medial temporal lobe in cognitively normal elderly. J. Neurosci. 35, 3240–3247.

Storandt, M., Mintun, M.A., Head, D., Morris, J.C., 2009. Cognitive decline and brain volume loss as signatures of cerebral amyloid-β peptide deposition identified with Pittsburgh Compound B: cognitive decline associated with Aβ deposition. Arch. Neurol. 66, 1476–1481.

Teipel, S.J., Meindl, T., Wagner, M., Stieltjes, B., 2010. Longitudinal changes in fiber tract integrity in healthy aging and mild cognitive impairment: a DTI follow-up study. J. Alzheimers Dis. 22, 507–522.

Tsao, S., Gajawelli, N., Hwang, D.H., Kriger, S., Law, M., Chui, H., Weiner, M., Lepore, N., 2014. Mapping of ApoE4 related white matter damage using diffusion MRI. Proc. SPIE Int.Soc. Opt. Eng. 9039, 90390H.

Vemuri, P., Lesnick, T.G., Przybelski, S.A., Knopman, D.S., Preboske, G.M., Kantarci, K., Raman, M.R., Machulda, M.M., Mielke, M.M., Lowe, V.J., Senjem, M.L., Gunter, J.L., Rocca, W.A., Roberts, R., Petersen, R.C., Jack Jr., C.R., 2015. Vascular and amyloid pathologies are independent predictors of cognitive decline in normal elderly. Brain 138, 761–771.

Villain, N., Fouquet, M., Baron, J.C., Mézenge, F., Landeau, B., la Sayette de, V., Viader, F., Eustache, F., Desgranges, B., Chételat, G., 2010. Sequential

relationships between grey matter and white matter atrophy and brain metabolic abnormalities in early Alzheimer's disease. Brain 133, 3301–3314.
Wakana, S., Jiang, H., Nagae-Poetscher, L.M., van Zijl, P.C.M., Mori, S., 2004. Fiber tract-based atlas of human white matter anatomy. Radiology 230, 77–87.
Wang, Y., West, J.D., Flashman, L.A., Wishart, H.A., Santulli, R.B., Rabin, L.A., Pare, N., Arfanakis, K., Saykin, A.J., 2012. Selective changes in white matter integrity in MCI and older adults with cognitive complaints. Biochim. Biophys. Acta 3, 423–430.
Ward, A.M., Schultz, A.P., Huijbers, W., Van Dijk, K.R.A., Hedden, T., Sperling, R.A., 2013. The parahippocampal gyrus links the default-mode cortical network with the medial temporal lobe memory system. Hum. Brain Mapp. 35, 1061–1073.
Westlye, L.T., Reinvang, I., Rootwelt, H., Espeseth, T., 2012. Effects of APOE on brain white matter microstructure in healthy adults. Neurology 79, 1961–1969.
Wu, M., Rosano, C., Butters, M., Whyte, E., Nable, M., Crooks, R., Meltzer, C.C., Reynolds III, C.F., Aizenstein, H.J., 2006. A fully automated method for quantifying and localizing white matter hyperintensities on MR images. Psychiatry Res. 148, 133–142.
Zhang, Y., Schuff, N., Jahng, G.H., Bayne, W., Mori, S., Schad, L., Mueller, S., Du, A.T., Kramer, J.H., Yaffe, K., Chui, H., Jagust, W.J., Miller, B.L., Weiner, M.W., 2007. Diffusion tensor imaging of cingulum fibers in mild cognitive impairment and Alzheimer disease. Neurology 68, 13–19.